The Journal of Chemical Physics

Vibrational energy transfer and anisotropy decay in liquid water: Is the Förster model valid?

Cite as: J. Chem. Phys. **135**, 164505 (2011); https://doi.org/10.1063/1.3655894
Submitted: 16 August 2011 . Accepted: 05 October 2011 . Published Online: 26 October 2011

Mino Yang, Fu Li, and J. L. Skinner


View Online


Export Citation

ARTICLES YOU MAY BE INTERESTED IN

IR and Raman spectra of liquid water: Theory and interpretation
The Journal of Chemical Physics **128**, 224511 (2008); https://doi.org/10.1063/1.2925258

Two-dimensional infrared spectroscopy and ultrafast anisotropy decay of water
The Journal of Chemical Physics **132**, 224503 (2010); https://doi.org/10.1063/1.3454733

IR spectral assignments for the hydrated excess proton in liquid water
The Journal of Chemical Physics **146**, 154507 (2017); https://doi.org/10.1063/1.4980121

AIP Publishing

© 2011 American Institute of Physics.

Vibrational energy transfer and anisotropy decay in liquid water: Is the Förster model valid?

Mino Yang,[1] Fu Li,[2] and J. L. Skinner[2,a)]
[1]*Department of Chemistry, Chungbuk National University, Cheongju, Chungbuk 361-763, South Korea*
[2]*Theoretical Chemistry Institute and Department of Chemistry, University of Wisconsin, Madison, Wisconsin 53706, USA*

(Received 16 August 2011; accepted 5 October 2011; published online 26 October 2011)

Ultrafast pump-probe anisotropy experiments have been performed on liquid H_2O and D_2O. In both cases, the anisotropy decay is extremely fast (on the order of 100 or 200 fs) and is presumed due to resonant vibrational energy transfer. The experiments have been interpreted in terms of the Förster theory, wherein the rate constant for intermolecular hopping transport is proportional to the inverse sixth power of the distance between the vibrational chromophores. In particular, the anisotropy decay is assumed to be simply related to the survival probability as calculated with the Förster theory. While the theory fits the data well, and is a reasonable model for these systems, there are several assumptions in the theory that might be suspect for water. Using our mixed quantum/classical model for vibrational spectroscopy and dynamics in liquid water, which agrees well with anisotropy decay experiments on the pure liquids as well as H_2O/D_2O mixtures, we critically analyze both the survival probability and anisotropy decay, in order to assess the applicability of the Förster theory. © *2011 American Institute of Physics*. [doi:10.1063/1.3655894]

I. INTRODUCTION

In an H_2O molecule in the gas phase, the two degenerate local-mode OH stretches are coupled, leading to a splitting between the symmetric and anti-symmetric OH stretch eigenstates. If one were to excite one quantum of one of the local modes, the excitation would oscillate in time back and forth between the two local modes. One would call this process coherent vibrational energy transfer. For an H_2O molecule in liquid water, due to perturbations from the surrounding molecules, the two OH local modes are no longer degenerate, and in addition, the intramolecular coupling is modified from its gas-phase value. Moreover, since the molecular environments are changing with time, the local-mode frequencies and intramolecular coupling fluctuate. If one were now to excite a local mode, the excitation would still transfer to the other local mode, but, because of the "bath" fluctuations, the energy transfer process is not necessarily coherent. In fact, the other limit of hopping or incoherent energy transfer might be a more appropriate description. In addition, in liquid water OH stretch vibrations on different molecules are coupled. Thus, a local OH stretch excitation on one molecule can transfer to OH stretches on nearby molecules. As in the above intramolecular example, whether the transfer is coherent or incoherent has to do with the strength and time scales of the bath fluctuations, and the time scale of interest.[1,2] Intramolecular and intermolecular OH stretch coupling in liquid water have been invoked to explain differences in polarized and depolarized Raman scattering and IR absorption.[3,4]

A much more dramatic manifestation of OH stretch vibrational coupling in liquid water is displayed by pump-probe anisotropy experiments. First consider the case of dilute HOD in D_2O. In this situation, because of the very large frequency mismatch between OH and OD stretches, the effect of vibrational coupling is minimal, and so, a state with one quantum of OH stretch is essentially an eigenstate of the vibrational Hamiltonian. Therefore, despite the vibrational coupling and fluctuations of the bath, an OH stretch excitation will not transfer to other stretches (although of course it will relax irreversibly to other lower frequency vibrational modes). Under these circumstances, a pump-probe anisotropy experiment, which measures time-dependent changes due to the chromophore's rotation, shows exponential decay (at least at long times), with an orientational relaxation time of 3 ps.[5,6] In contrast, in pure H_2O, the anisotropy decay time scales are between 100 and 200 fs (Refs. 7 and 8)—roughly twenty times shorter. This faster decay is due to intramolecular and intermolecular vibrational energy transfer, as this provides another mechanism for changing chromophores' orientations. Recent experiments have also measured pump-probe anisotropy decays in pure D_2O, and H_2O/D_2O mixtures, focusing now on the OD stretch.[9] For the mixtures, hydrogen exchange produces nearly statistical mole fractions of H_2O, HOD, and D_2O. As might be anticipated, the anisotropy decay curves change continuously from slow nearly exponential decay at very low D_2O concentrations (dilute HOD in H_2O), to fast decay in neat D_2O.

These fascinating and important anisotropy decay experiments have been interpreted[7,9] in terms of Förster energy transfer.[10] The Förster theory was developed to describe electronic excitation transfer between an initially excited donor molecule and randomly distributed acceptors.[1,2,11–18] Assuming that the rate constant for incoherent hopping between a donor-acceptor pair is $k = (1/\tau)(r_o/r)^6$, where τ is the

a)Author to whom correspondence should be addressed. Electronic mail: skinner@chem.wisc.edu.

 © 2011 American Institute of Physics

excitation lifetime, r is the donor-acceptor distance, and r_o is the so-called Förster radius, one then sets up a master equation for this problem, and finds that the average probability of remaining on the donor (survival probability) at time t is

$$S(t) = \exp\left(-\frac{4\pi^{3/2}\rho r_o^3}{3}\sqrt{\frac{t}{\tau}}\right), \quad (1)$$

where ρ is the number density of acceptors. This beautifully simple formula shows a characteristic non-exponential decay.

If the acceptors are not only randomly distributed in space (in relation to the donor), but also randomly oriented (in relation to the orientation of the donor), then energy transfer will lead to no anisotropy from the acceptors, and all the anisotropy will be due to the originally excited donor. In this case, the anisotropy is simply proportional to the donor survival probability discussed above. Of course, the physical rotations of molecules also lead to anisotropy decay.[19] If this is exponential, then one would write

$$r(t) = \frac{2}{5}e^{-t/\tau_{or}}S(t), \quad (2)$$

where $r(t)$ is the time-dependent anisotropy, τ_{or} is the orientation relaxation time, and $S(t)$ is the above survival probability. This formula was able to describe the above anisotropy experiments quite well, with a Förster radius on the order of 2 Å.[7,9]

The fact that this formula fits these experiments is a bit puzzling, since it is not obvious that the assumptions of the theory are fulfilled by the circumstances of these experiments. First of all, as correctly noted by Piatkowski *et al.*,[9] the orientations of the OH acceptors are not random with respect to the donor, but rather reflect the hydrogen-bonding structure of the liquid. Therefore, it seems likely that there are contributions from the acceptor molecules to the anisotropy, which are not taken into account with this formula. In addition, there are questions about the Förster expression (Eq. (1)) for the survival probability itself, and its appropriateness for vibrational energy transfer in water. For example, the Förster theory assumes irreversible donor-acceptor transfer, whereas in these resonant experiments the excitation can move back to the original site; the Förster theory assumes that the acceptors are randomly distributed, whereas in liquid water this is not the case; the Förster theory pre-averages the orientation dependence of the energy transfer rate constant. Moreover, the Förster theory assumes incoherent hopping, while, as alluded to above, at short times and distances this may not be the correct picture; Förster theory uses perturbation theory to arrive at the $1/r^6$ dependence of the rate constant, which is not necessarily valid. Finally, in water there is the possibility of intramolecular energy transfer, which also contributes to the anisotropy decay, and is not taken into account by Förster theory.

We have developed a theory of vibrational spectroscopy and dynamics in liquid water where the stretching degrees of freedom are treated quantum mechanically, and the bath degrees of freedom (translations and rotations) are treated classically.[20] The parameters in the spectroscopic one-exciton Hamiltonian are deduced from electronic structure calculations on water clusters, and the motion of the bath is obtained from classical molecular dynamics simulations. We have applied the theory to water in a number of different circumstances (isotopically dilute and pure liquids,[3,21,22] ice,[23,24] liquid-vapor interface,[25–28] salt solutions,[29] and confined in reverse micelles[30] and lipid multi-bilayers[31]). Together with Thomas Jansen, we have also used the theory to calculate the anisotropy decay in H_2O,[32] obtaining reasonable agreement with experiment.[7,8]

In this paper, using this theoretical model we calculate the anisotropy decay for the OD stretch in H_2O/D_2O mixtures.[9] We find that our results are in reasonable agreement with experiment. This, in addition to our previous comparison with experiment for pure H_2O,[32] validates our theoretical model, meaning, we think it provides a qualitatively correct picture of the energy transfer dynamics. To the extent that this is true, this allows us to analyze our theoretical results in order to address some of the above puzzles. For definiteness, we focus on pure water. The organization of this paper is as follows. In Sec. II, we set up the vibrational exciton Hamiltonian, derive expressions for the anisotropy from the third-order response functions, and show under what conditions the anisotropy is proportional to the survival probability. In Sec. III, we compare our theoretical results to experiments for the H_2O/D_2O mixtures and pure water. In addition, we investigate the validity of the product form as in Eq. (2) for the anisotropy decay, and the validity of the Förster formula for the survival probability. We find that the product form is not valid, because it neglects the anisotropy of the acceptors, and that by including reversible energy transfer and taking into account non-random positions and orientations of the acceptors, we can generalize the Förster theory and obtain results in good agreement with our exact survival probability. In Sec. IV, we conclude with a general discussion of the title question.

II. THEORY

A. One-exciton Hamiltonian

As mentioned above, we treat OH (OD) vibrations quantum mechanically. We write the one-exciton Hamiltonian (for the manifold of single excitations) in the site (local-mode) basis as

$$H(t) = \sum_i \hbar\omega_i(t)|i\rangle\langle i| + \sum_{i,j}\hbar\omega_{ij}(t)|i\rangle\langle j|. \quad (3)$$

$|i\rangle$ is the state of the system with a single excitation on chromophore i, and the sums run from 1 to N, where N is the number of OH (OD) chromophores. Thus, ω_i are the site frequencies, and ω_{ij} are the vibrational couplings, with $\omega_{ii} = 0$ by definition. If i and j represent chromophores on the same molecule, then this is an intramolecular coupling element, ω_{ij}^a, while if i and j are on different molecules, this is an intermolecular coupling element ω_{ij}^e. As discussed earlier, in our mixed quantum/classical approach, the bath variables, which affect this one-exciton Hamiltonian, are treated classically, which leads to fluctuating matrix elements as shown and, thus, a time-dependent Hamiltonian $H(t)$.

The site frequencies are given by frequency "maps", which have been determined for both the OH and OD

stretches, and depend on the local electric field.[3,20,21,29] In what follows, we will use the SPC/E simulation model,[33] and these maps are appropriate for this model. ω_{ij}^{a} is determined by a more complicated map, which depends on local electric fields, as well as position and momentum matrix elements for each local mode, and which have themselves been parameterized in terms of local-mode frequencies.[28] The intermolecular coupling is taken to be of the transition dipole-transition dipole form. The transition dipole for an OH (OD) stretch is in the direction of the OH (OD) bond, and is centered along the bond at a point 0.58 Å from the O to the H (D). For the ith chromophore, the transition dipole vector is $\vec{\mu}_i = m_i \hat{u}_i$, where m_i is the magnitude and $\hat{u}_i$ is the OH (OD) bond unit vector. $m_i = \mu' x_i$, where μ' is the dipole derivative, and x_i is the above-mentioned position matrix element. The dipole derivative is also parameterized in terms of the local electric field. The intermolecular coupling frequency is therefore given by

$$\hbar\omega_{ij}^{e} = \frac{\kappa_{ij}}{r_{ij}^{3}} m_i m_j, \tag{4}$$

where κ_{ij} is the orientation factor defined by

$$\kappa_{ij} = \hat{u}_i \cdot \hat{u}_j - 3(\hat{u}_i \cdot \hat{r}_{ij})(\hat{u}_j \cdot \hat{r}_{ij}), \tag{5}$$

where r_{ij} is the distance between the chromophores, and $\hat{r}_{ij}$ is the unit vector from the position of one transition dipole to the other.

Suppose that the initial state of the system is an excitation on site i: $|i\rangle$. The state vector at a time t later is given by $U(t)|i\rangle$, where $U(t)$ is the propagator, which obeys the time-dependent Schrödinger equation

$$\dot{U}(t) = -\frac{i}{\hbar} H(t) U(t). \tag{6}$$

The amplitude for finding the excitation on site j at time t, for a particular trajectory, is then $\langle j|U(t)|i\rangle \equiv U_{ji}(t)$. The average probability of finding the excitation on site j at time t, given that it was initially on site i, is $P_{ji}(t) = \langle |U_{ji}(t)|^2 \rangle$, where the brackets denote an average over an ensemble of trajectories. The average survival probability is, therefore,

$$S(t) = \frac{1}{N} \sum_{i=1}^{N} P_{ii}(t). \tag{7}$$

B. Pump-probe anisotropy decay

For the ultrafast vibrational pump-probe experiments, the anisotropy decay is constructed by[19,34–37]

$$r(t) = \frac{I^{\parallel}(t) - I^{\perp}(t)}{I^{\parallel}(t) + 2I^{\perp}(t)}, \tag{8}$$

where $I^{\parallel}(t)$ is the absorption change when the probe is parallel to the pump, $I^{\perp}(t)$ is the absorption change when the probe is perpendicular to the pump, and t is the time delay between the pump and probe.

The absorption changes can be calculated from the third-order response functions.[38,39] For the pump-probe experiment, these are listed in Appendix A. Assuming impulsive excitation, frequency-integrated detection, and making the very reasonable assumptions that the transition dipole for the 1–2 transition of chromophore i is proportional to $\vec{\mu}_i$ (for the 0–1 transition) and that certain interference terms can be neglected, the result (see Appendix A) is

$$r(t) = \frac{2}{5} \frac{\left\langle \sum_j m_j(t)^2 |U_{ji}(t)|^2 m_i(0)^2 P_2(\hat{u}_i(0) \cdot \hat{u}_j(t)) \right\rangle_i}{\left\langle \sum_j m_j(t)^2 |U_{ji}(t)|^2 m_i(0)^2 \right\rangle_i}, \tag{9}$$

where P_2 is the second Legendre polynomial, and the average is over all trajectories, and as indicated, over all initially excited states i.

If there is no energy transfer then $U_{ji}(t) = \delta_{ij}$, and we obtain

$$r_{\mathrm{rot}}(t) = \frac{2}{5} \frac{\langle m_i(t)^2 m_i(0)^2 P_2(\hat{u}_i(0) \cdot \hat{u}_i(t)) \rangle_i}{\langle m_i(t)^2 m_i(0)^2 \rangle_i}, \tag{10}$$

as derived previously.[22] As indicated by the subscript "rot," in this case the anisotropy decay is due to rotation only. Note, also, that within the Condon approximation[40] ($m_i(t)$ is a constant), one recovers the usual result that

$$r_{\mathrm{rot}}(t) = \frac{2}{5} \langle P_2(\hat{u}_i(0) \cdot \hat{u}_i(t)) \rangle_i . \tag{11}$$

In order to make the connection between the anisotropy decay and survival probability, we first note that if the transition dipoles for the final states j in Eq. (9) are randomly oriented with respect to $\hat{u}_i$, all terms in the numerator of Eq. (9) will vanish except that with $j = i$. Taking only this term and also assuming that the statistical averages factor in both numerator and denominator, we obtain

$$r(t) = \frac{2}{5} \frac{\langle m_i(t)^2 m_i(0)^2 P_2(\hat{u}_i(0) \cdot \hat{u}_i(t)) \rangle_i \langle |U_{ii}(t)|^2 \rangle_i}{\sum_j \langle m_j(t)^2 m_i(0)^2 \rangle_i \langle |U_{ji}(t)|^2 \rangle_i}. \tag{12}$$

Finally, if we make the assumption that $\langle m_j(t)^2 m_i(0)^2 \rangle = \langle m_i(t)^2 m_i(0)^2 \rangle$ for all i and j, then, using the fact that $\sum_j |U_{ji}(t)|^2 = 1$, we obtain

$$r(t) = r_{\mathrm{rot}}(t) S(t), \tag{13}$$

where $r_{\mathrm{rot}}(t)$ is given by Eq. (10). If $r_{\mathrm{rot}}(t)$ is taken to be exponential, and the Förster expression Eq. (1) for the survival probability is assumed, one obtains Eq. (2), which was used in the analysis of experimental data.[9]

C. Molecular dynamics simulations

To implement the mixed quantum/classical approach discussed above, molecular dynamics simulations were performed on 128 SPC/E water (H_2O) molecules in the *NVE* ensemble at 298 K with the experimental density. The integration time step of the simulation was 1 fs and every 10 fs all atomic coordinates were saved to generate a 2 ns atomic trajectory. From the trajectory, we determined the electric field along every individual dipole direction, and then by using the mapping relations in Table I,[3,21,28,29] the time-dependent Hamiltonian matrix elements. Equation (6) was integrated numerically for each of the initially excited chromophores, and for a new starting configuration every 1 ps. These results

TABLE I. Maps for the transition frequencies, ω, position and momentum matrix elements, x and p, respectively, intramolecular coupling frequencies, ω^a_{ij}, and dipole derivative, μ'.[3,28,29] Frequencies are in cm^{-1} and all other quantities are in atomic units.

$\omega_{OH} = 3762 - 5060E - 86225E^2$
$\omega_{OD} = 2762.6 - 3640.8E - 56641E^2$
$x_{OH} = 0.1934 - 1.75 \times 10^{-5}\omega_{OH}$
$x_{OD} = 0.16627 - 2.0884 \times 10^{-5}\omega_{OD}$
$p_{OH} = 1.611 + 5.893 \times 10^{-4}\omega_{OH}$
$p_{OD} = 1.9844 + 9.1907 \times 10^{-4}\omega_{OD}$
$\omega^a_{ij} = (-1789 + 23852(E_i + E_j))x_i x_j - 1.966 p_i p_j$
$\mu' = 0.1333 + 14.17E$

were then averaged appropriately to calculate the various observables.

For the D_2O/H_2O mixtures at a certain mole fraction X of D_2O, for the purpose of the anisotropy calculations, H atoms were randomly assigned to be D atoms with probability X. The exciton Hamiltonian, therefore, has NX OD chromophores.

III. RESULTS AND DISCUSSION

The main goal of this paper is to assess the appropriateness of the Förster model for anisotropy decay experiments in water. To this end, we first compare our theoretical results to experiment. The purpose here is primarily to validate the theoretical model. Subsequently, we will analyze our theoretical results.

A. Anisotropy decay and comparison to experiment

We begin by considering the recent experiments involving the OD stretch of H_2O/D_2O mixtures.[9] Anisotropy decays were measured at D_2O concentrations ranging from 1% to 100%. Note that in the former case, this corresponds approximately to a 2% solution of HOD in H_2O, which is close to the dilute limit.[9] The experimental data are shown in Fig. 1. The low-concentration result shows, after an initial drop, nearly exponential decay, with a time constant of 2.6 ps, corresponding to rotational dynamics of individual molecules.[9] As the D concentration increases, the anisotropy decreases more quickly due to vibrational energy transfer. For the neat D_2O liquid, the anisotropy has decayed to roughly 10% of its initial value in 200 fs.

Also shown in the figure are our calculated results for the anisotropy decay, using Eq. (9). Comparison between theory and experiment shows that the theory does quite well, clearly capturing the correct concentration dependence and showing virtually quantitative agreement with experiment for the neat liquid. The discrepancy between theory and experiment at low D concentration is presumably mainly due to the fact that in experiment the anisotropy decay is frequency-resolved (near the OD stretch band maximum), while the theory is for the frequency-integrated case. We have shown previously that this distinction can make a significant difference,[22] which reflects the effects of vibrational coherence during the detection period, and which we believe is most significant in the low-concentration limit (since for the neat liquid the energy transfer process dominates the anisotropy decay, and so, the difference between the frequency-integrated and frequency-resolved curves should be diminished). For the low-concentration limit, in Fig. 1 we also show our result for the frequency-resolved decay,[22] which is indeed in better agreement with experiment. We note here that performing frequency-resolved theoretical calculations when not in the dilute limit is possible, but much more complicated due to the involvement of the two-exciton states.[32,41,42]

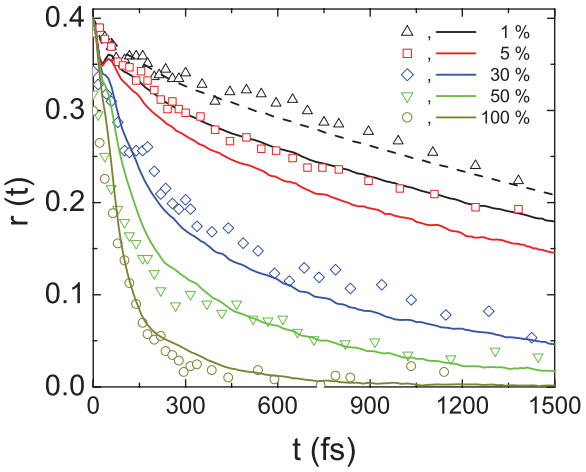

FIG. 1. Theoretical and experimental anisotropy decay for OD stretch excitation in D_2O/H_2O mixtures at different deuterium mole fractions. The theoretical curves are calculated from Eq. (9). The dashed line is the frequency-resolved result for the lowest concentration.[22]

Anisotropy decay in pure H_2O was also measured a decade ago by Bakker and coworkers,[7] and more recently by Miller and coworkers.[8] In Fig. 2, we show the latter results, which are for the frequency-integrated anisotropy, scaled so the initial value is 0.4, and also the earlier results. These results are similar to those for D_2O. In the figure, we also show our theoretical results for H_2O. These are numerically identical to those obtained independently (with a different code) in

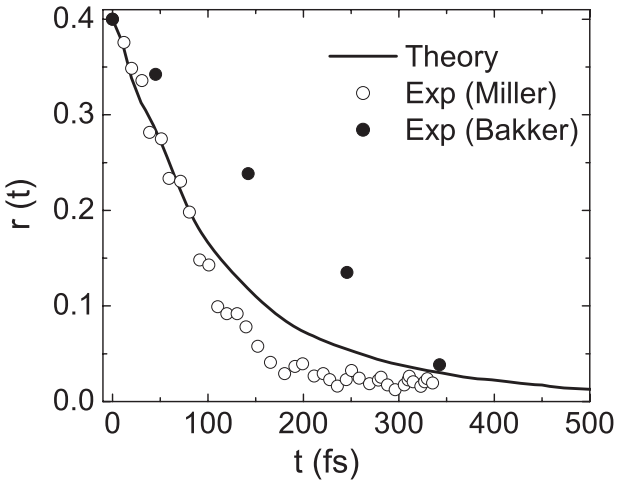

FIG. 2. Theoretical and experimental (Miller and coworkers[8] at 304 K and Woutersen and Bakker[7] at 298 K) anisotropy decay for OH stretch excitation in pure H_2O. The theoretical curve (for 298 K) is calculated from Eq. (9).

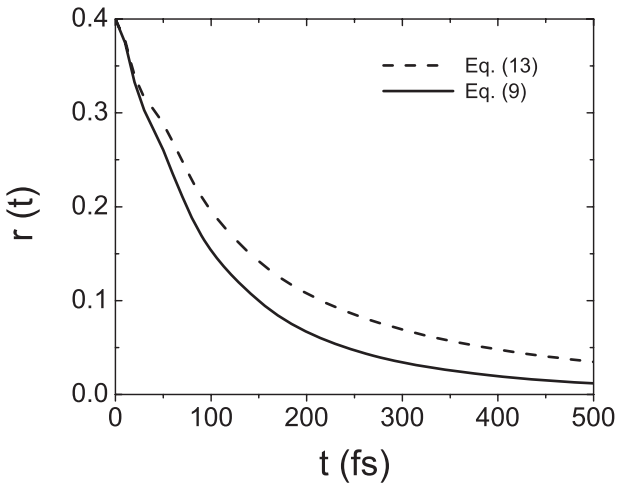

FIG. 3. Comparison of the exact anisotropy (solid, Eq. (9)), and the product form (dashed, Eq. (13)).

our previous paper.[32] Agreement between theory and experiment is again satisfactory.

Although our results are not in perfect agreement with experiment, we consider them good enough to validate the theoretical model we use, in the sense that we believe the model describes the correct physics. From now on, then, we will analyze these theoretical results. For definiteness, we will consider only the case of neat liquid H_2O.

B. Is the anisotropy decay proportional to the survival probability?

The first question in investigating the appropriateness of the Förster model is to assess the validity of Eq. (13). As we have seen above, derivation of this equation, independent of the Förster model for the survival probability, already rests on a number of approximations.

To this end, we calculate the rotational contribution to the anisotropy decay from Eq. (10) and the survival probability from Eq. (7), and compare their product, as in Eq. (13), to the exact anisotropy decay from Eq. (9). This comparison is shown in Fig. 3. One sees that in fact the product approximation, while qualitatively correct, significantly overestimates the anisotropy by as much as a factor of 2 at $t = 0.3$ ps. This discrepancy is due either to the neglect of terms with $j \neq i$ in Eq. (9), to the factorization of the statistical averages (as in Eq. (12)), or to the equality of the non-Condon fluctuations ($\langle m_j(t)^2 m_i(0)^2\rangle = \langle m_i(t)^2 m_i(0)^2\rangle$ for all i and j), and indeed, most likely to all three. The first approximation is suspect because the nearby acceptors (especially the intramolecular one) are *not* randomly oriented, the factorization approximation is suspect because $|U_{ji}(t)|^2$ depends on the fluctuating quantities $m_i(t)$ and $\hat{u}_i(t)$ through the intermolecular coupling (see Eqs. (4) and (5)), and the last approximation is suspect because $m_i(0)$ and $m_i(t)$ are likely to be strongly correlated, while $m_i(0)$ and $m_j(t)$ are less so. Given this, it is perhaps not so surprising that the product form of Eq. (13) is not quantitatively correct. Again, this conclusion is independent of the Förster model for the survival probability.

C. The Förster model for the survival probability

Our next step is to assess the validity of the Förster model for calculating the survival probability. The starting point for the derivation of Eq. (1) for the survival probability is an expression for the rate constant for incoherent energy transfer between a pair of chromophores due to dipole-dipole coupling[14]

$$k_{ij} = \frac{3}{2}\frac{\kappa_{ij}^2}{\tau}\left(\frac{r_o}{r_{ij}}\right)^6, \tag{14}$$

where κ_{ij} is the orientation factor in Eq. (5), r_{ij} is the distance between the chromophores, r_o is the Förster radius, and τ is the chromophores' lifetime.

In order to compare the results of Eq. (1) to our calculated survival probability from Eq. (7), we need to be able to determine r_o^6/τ from our simulations. Equation (14) comes from perturbation theory in the vibrational coupling. Within the context of our Hamiltonian, first-order time-dependent perturbation theory shows that the rate constant for incoherent hopping from chromophore i on one molecule to chromophore j on another is given by[1,15]

$$k_{ij} = 2Re\int_0^\infty dt\,\left\langle \omega_{ij}^e(t)\omega_{ij}^e(0)e^{i\int_0^t d\tau\,(\omega_i(\tau)-\omega_j(\tau))}\right\rangle. \tag{15}$$

Substituting in Eq. (4), and assuming that the distance and orientation between the chromophores are approximately constant (on the time scale of the decay of the integrand), we obtain

$$k_{ij} = \frac{2\kappa_{ij}^2}{\hbar^2 r_{ij}^6} Re\int_0^\infty dt\,\langle m_i(t)m_j(t)m_i(0)m_j(0)e^{i\int_0^t d\tau\,(\omega_i(\tau)-\omega_j(\tau))}\rangle. \tag{16}$$

If the two chromophores are nearby in space, then $m_i(t)$ and $\omega_i(t)$ will be correlated with $m_j(t)$ and $\omega_j(t)$, but if the chromophores are sufficiently far apart, they will be uncorrelated, in which case

$$k_{ij} = \frac{2\kappa_{ij}^2}{\hbar^2 r_{ij}^6} Re\int_0^\infty dt\,\langle m_i(t)m_i(0)e^{i\int_0^t d\tau\,\omega_i(\tau)}\rangle \times\langle m_j(t)m_j(0)e^{-i\int_0^t d\tau\,\omega_j(\tau)}\rangle. \tag{17}$$

Comparing Eqs. (14) and (17), it follows that

$$\frac{r_o^6}{\tau} = \frac{4}{3\hbar^2}\int_0^\infty dt\,|\langle m_i(t)m_i(0)e^{i\int_0^t d\tau\,\omega_i(\tau)}\rangle|^2. \tag{18}$$

We note in passing that this can be written as the convolution of identical donor and acceptor absorption line shapes, which is consistent with other treatments of Förster transfer (assuming a classical bath).[1,15] The right-hand side of this equation can easily be computed from our simulations, for both OH and OD stretches. Using the isolated-chromophore lifetimes of $\tau = 0.74$ ps and 1.7 ps,[5,6,19,43] we obtain values of $r_0 = 2.07$ Å and $r_0 = 2.27$ Å for H_2O and D_2O, respectively. These two values are remarkably close to the ones (2.10 $\pm$ 0.05 Å and 2.3 $\pm$ 0.2 Å, respectively) obtained from fitting to experiment.[7,9]

We now compare our calculated survival probability from the simulation (Eq. (7)) to the Förster result (Eq. (1)) using the above value of r_o^6/τ for H_2O in Fig. 4. One sees that

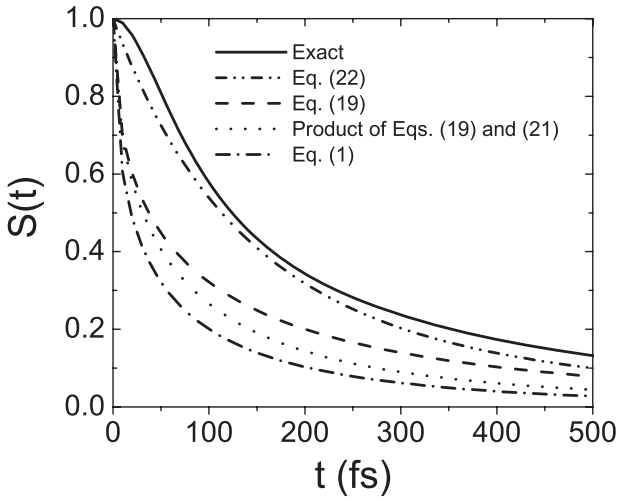

FIG. 4. Different approximations to the survival probability, compared to the exact result (solid) from Eq. (7). The Förster result (dashed–dotted) is from Eq. (1). The Förster result for reversible intermolecular energy transfer (long dashed) is from Eq. (19). The result including intramolecular energy transfer (dotted) is from the product of Eqs. (19) and (21). Our best approximation (dashed-dotted-dotted) is from Eq. (22).

the Förster model shows a very significantly smaller survival probability than that calculated directly numerically from our model. This provides a partial explanation for why the Förster model can fit the experimental data: while the product form for the anisotropy decay is too high, the Förster result for the survival probability is too low, and these two errors, therefore, cancel each other to some extent.

D. Extending the Förster model for water

As mentioned in the Introduction, there are a number of reasons why the Förster model might not work for liquid water. Several of these become clear from understanding the details of the derivation of the Förster result. Therefore, starting from Eq. (14), in Appendix B we provide a simple derivation of Eq. (1). From this, it is clear that the result depends on, in addition to the underlying assumption of perturbation theory for the rate constant, assumptions of irreversible and incoherent donor-acceptor energy transfer, static and random (including infinitely close) acceptor positions, and pre-averaging the orientational factor in the rate constant. In addition, the Förster result does not include intramolecular energy transfer. In this section, we will explore modifications to the Förster result based on these considerations.

1. Reversible energy transfer

If the intermolecular vibrational energy transfer is irreversible, solution of the master equation for a given configuration is trivial, as described in Appendix B. However, for resonant vibrations energy transfer is reversible, in which case solution of the master equation is much more complicated.[16–18] One simple approximation solves the master equation exactly for a donor-acceptor pair and, then, assumes a product form for the survival probability,[14,18] as described briefly in Appendix C, in which case the Förster result becomes

$$S(t) = \exp\left(-\frac{(2\pi)^{3/2}\rho r_o^3}{3}\sqrt{\frac{t}{\tau}}\right). \tag{19}$$

Note that this is identical to the Förster result for irreversible energy transfer (Eq. (1)) except for division by a factor of $\sqrt{2}$ in the exponent. Reversible energy transfer obviously increases the survival probability. This result is also shown in Fig. 4. Although it is larger than the result for irreversible energy transfer, it is still significantly smaller than the exact result.

2. Intramolecular energy transfer

In liquid water, in addition to intermolecular energy transfer, there is also intramolecular energy transfer, which is neglected in the Förster model. Assuming perturbation theory is valid, and that the bath fluctuations lead to incoherent hopping, we can estimate the rate constant for intramolecular energy transfer from[1,15]

$$k_a = 2Re\int_0^\infty dt\,\langle\omega_{ij}^a(t)\omega_{ij}^a(0)e^{i\int_0^t d\tau\,(\omega_i(\tau)-\omega_j(\tau))}\rangle. \tag{20}$$

From the simulation, we determine this to be $k_a = 2.08\ \text{ps}^{-1}$.

Assuming only intramolecular energy transfer, the survival probability for an initially excited donor is

$$S_a(t) = \frac{1}{2}(1 + e^{-2k_a t}), \tag{21}$$

and so, in the spirit of Appendix C, a simple approximation to the survival probability, including reversible intermolecular energy transfer, and intramolecular energy transfer, is the product of Eqs. (19) and (21). This result is also shown in Fig. 4. This result is, of course, smaller than that for Eq. (19) since now an additional relaxation channel is opened.

3. Non-uniform distribution of acceptors and pre-averaging the orientation factor

As seen above, including reversible intermolecular and intramolecular energy transport, the extended Förster result still decays much faster than the exact survival probability. One important reason for this is that the usual Förster result assumes that the acceptors have random positions. Of course, this is not the case in liquid water, where repulsive intermolecular interactions insure that molecules never get too close together. In Fig. 5, we show the radial distribution function $g(r)$ for the transition dipole positions. The graph shows some structure due to hydrogen bonding, but the most important effect is that acceptors are excluded within 2 Å of the donor. If this distance were small compared to r_o, as it often is in the electronic case, then it would not be important. But, in this case it is on the order of r_o, and so it becomes very important.

Another approximation made in the Förster theory is to pre-average the orientation factor, as discussed earlier. In fact, because of the hydrogen-bonding structure of the liquid, the average orientation factor depends on distance. Thus, in pre-averaging this orientation factor, one should really do it

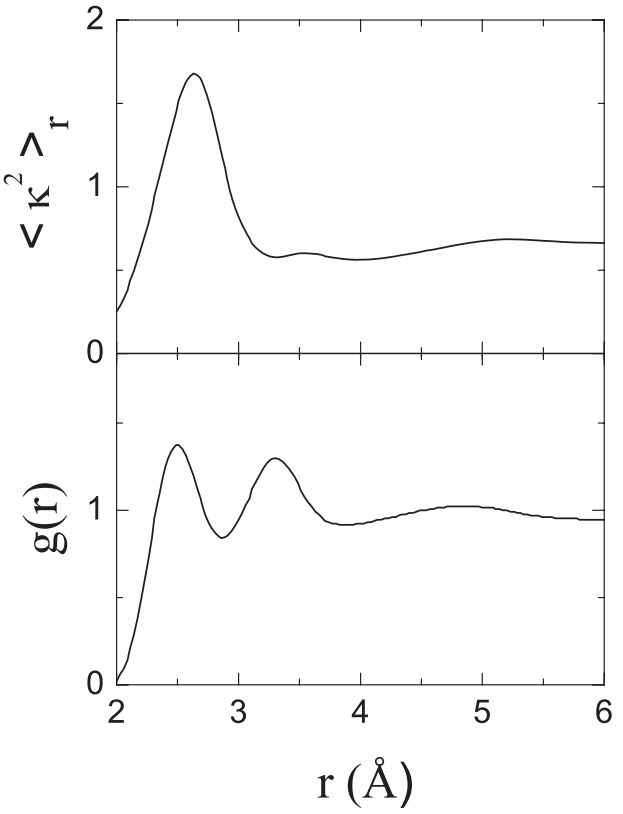

FIG. 5. Distance-dependent average of orientation factor $\langle \kappa^2 \rangle_r$ and pair correlation function $g(r)$ for intermolecular OH dipole positions.

separately for each r, to obtain $\langle \kappa^2 \rangle_r$. This is also shown in Fig. 5, where one sees that for chromophore pairs within 3 Å, $\langle \kappa^2 \rangle_r$ is substantially larger than the average (2/3) for random orientations.[14]

Both of these features can be taken into account in a further generalized Förster result, as described in Appendix D. Assuming reversible intermolecular transport, and including intramolecular transport as well, our final result is

$$S(t) = S_a(t) \exp\left(-2\pi\rho \int_0^\infty r^2 g(r) dr (1 - e^{-(t/\tau)3\langle \kappa^2 \rangle_r (r_o/r)^6})\right). \quad (22)$$

Using $\langle \kappa^2 \rangle_r$ and $g(r)$ from Fig. 5, this can be integrated numerically, and the results are also shown in Fig. 4. One sees that now, except at very short times, this result is in good agreement with the exact survival probability. Note that the exclusion due to repulsive interactions is generally (and in this case) more important than the distance-dependent pre-averaging.

IV. CONCLUDING REMARKS

The title question "Is the Förster model valid?" really has two parts. One part concerns the validity of the Förster Eq. (1) for describing the survival probability of an initially excited OH stretch in liquid water. To answer this question, we use the theoretical model we have developed for vibrational spectroscopy and dynamics in liquid water. Within the model, which, based on comparison of its results to many experiments including those discussed herein, we believe provides a qualitatively correct description, the answer is no. The Förster model survival probability decays much too quickly. However, the model can be extended to include reversible energy transfer, and to take into account the non-random (with respect to an OH donor) spatial and orientational distributions of OH acceptors. If, in addition, intramolecular energy transfer is included, then the extended Förster model really works quite well.

The second part concerns the validity of the product approximation Eq. (2), or slightly more generally, Eq. (13), which states that the anisotropy decay is proportional to the survival probability. Here, again we find that the product approximation is not valid. It seems most likely that this again is due to the incorrect assumption of randomly oriented acceptors. In fact, because of the tetrahedral hydrogen-bonding structure of the liquid, the typical angle between donors and nearby intermolecular acceptors is $\theta \simeq 70.5^\circ$, while for the intramolecular acceptor it is 109.5°. In both cases, $P_2(\theta) = -1/3$, which means that the anisotropy of these acceptors is non-zero, and in fact, is negative. By neglecting this anisotropy (while using the product form), one obtains a result that is too large, as in Fig. 3. From this analysis, it is clear, at least in part, why Eq. (2) could provide a good fit to the anisotropy experiments: there is a cancellation of errors, in that the product form produces too large a result, and the Förster form gives too small a result.

Two other points, alluded to in the Introduction, also merit comments. First, the Förster rate constant is based on perturbation theory in the vibrational coupling. Using perturbation theory, we calculated this rate constant from our simulations, and then, we used the result in our subsequent analysis. Our final results for the survival probability are in good agreement with exact results, which would suggest, but certainly does not prove, that perturbation theory suffices. Second, Förster energy transfer is an incoherent hopping process, and as such is described by a master equation. Is the energy transfer really incoherent? Again, agreement of our hopping model with exact results would suggest that it is (at least for the survival probability). However, a careful inspection of Fig. 4 shows that at short times the hopping model survival probability of Eq. (22) decays too quickly and has a cusp at $t = 0$, whereas the exact result does not have a cusp. The vanishing slope at $t = 0$ for the exact result is a signature of coherent transport. And indeed, in a previous paper,[4] we analyzed the Raman line shapes in H_2O as arising from coherent energy transfer. So, really, the question of coherent or incoherent transport is one of time scales. In Raman spectroscopy, the relevant time scale is roughly 50 fs,[4] at which point the transport is still coherent, whereas for the survival probability the relevant time scale is more like 200 fs, and the transport is incoherent.

ACKNOWLEDGMENTS

J.L.S. acknowledges support from the NSF (CHE-1058752) for development of the analytical results, and support from the DOE (DE-FG02-09ER16110) for molecular dynamics simulations and numerical calculations. M.Y.

acknowledges support from the research grant of Chungbuk National University in 2009.

APPENDIX A: DERIVATION OF THE ANISOTROPY DECAY

The third-order response functions for pump-probe experiments, with impulsive excitation and frequency-integrated detection, are[39]

$$R_{\mathrm{GB}}^{ppp'p'}(t) = \left\langle \langle 0|\, \mu_{01}^{p}(0)\mu_{10}^{p}(0)\mu_{01}^{p'}(t)\mu_{10}^{p'}(t)\, |0\rangle \right\rangle, \tag{A1}$$

$$R_{\mathrm{SE}}^{ppp'p'}(t) = \left\langle \langle 0|\, \mu_{01}^{p}(0)U^{\dagger}(t)\mu_{10}^{p'}(t)\mu_{01}^{p'}(t)U(t)\mu_{10}^{p}(0)\, |0\rangle \right\rangle, \tag{A2}$$

$$R_{\mathrm{EA}}^{ppp'p'}(t) = -\left\langle \langle 0|\, \mu_{01}^{p}(0)U^{\dagger}(t)\mu_{12}^{p'}(t)\mu_{21}^{p'}(t)U(t)\mu_{10}^{p}(0)\, |0\rangle \right\rangle, \tag{A3}$$

where GB, SE, and EA correspond, respectively, to ground-state bleach, stimulated emission, and excited-state absorption, $U(t)$ is the time-evolution operator from Eq. (6), and $|0\rangle$ is the quantum state with no excitations. $\mu_{10}^{p}(t)$ is the component in the direction $\hat{p}$ (the light polarization direction) of the transition dipole operator between the ground state and the one-exciton states

$$\mu_{10}^{p}(t) = \sum_{i} \mu_{i}^{p}(t)|i\rangle\langle 0|, \tag{A4}$$

where $\mu_{i}^{p}(t) = \vec{\mu}_{i}(t)\cdot\hat{p}$, and $\mu_{21}^{p}(t)$ is the same for the transition dipole operator between the one-exciton and two-exciton states

$$\mu_{21}^{p}(t) = \sum_{i} \bar{\mu}_{i}^{p}(t)\left|\bar{i}\right\rangle\langle i| + \sum_{i\neq j} \mu_{j}^{p}(t)\,|ij\rangle\,\langle i|\,. \tag{A5}$$

The first term in this equation corresponds to transitions from single to double excitations $\left|\bar{i}\right\rangle$ on the same chromophore, with transition dipole component $\bar{\mu}_{i}^{p}$, while the second term corresponds to pairs of single excitations $|ij\rangle$.

First, let us consider the matrix element

$$\langle i|\, \mu_{12}^{p'}\mu_{21}^{p'}\,|j\rangle = \mu_{i}^{p'}\mu_{j}^{p'} + \delta_{ij}\left[\left(\bar{\mu}_{i}^{p'}\right)^{2} - 2\left(\mu_{i}^{p'}\right)^{2}\right] + \delta_{ij}\sum_{k}\left(\mu_{k}^{p'}\right)^{2}. \tag{A6}$$

Inserting this into Eq. (A3) for the EA response function gives three terms, the first and last of which are identical (but with the opposite sign) to the SE and GB response functions, respectively. Therefore, when one determines the absorption change $I^{ppp'p'}(t)$, from the sum of the response functions,[44] $I^{ppp'p'}(t) = R_{\mathrm{GB}}^{ppp'p'}(t) + R_{\mathrm{SE}}^{ppp'p'}(t) + R_{\mathrm{EA}}^{ppp'p'}(t)$, one obtains simply

$$I^{ppp'p'}(t) = \sum_{ijk}\left\langle \mu_{i}^{p}(0)U_{ij}^{\dagger}(t)\left[2\mu_{j}^{p'}(t)^{2} - \bar{\mu}_{j}^{p'}(t)^{2}\right]U_{jk}(t)\mu_{k}^{p}(0)\right\rangle. \tag{A7}$$

This can also be written as

$$I^{ppp'p'}(t) = \sum_{j}\left\langle \left|\sum_{i}\mu_{i}^{p}(0)U_{ji}(t)\right|^{2}\left[2\mu_{j}^{p'}(t)^{2} - \bar{\mu}_{j}^{p'}(t)^{2}\right]\right\rangle. \tag{A8}$$

Note that if the system is harmonic, $\bar{\mu}_{j}^{p'} = \sqrt{2}\mu_{j}^{p'}$, and the signal will vanish. More generally, this equation can be simplified by making the reasonable assumption that $\bar{\mu}_{j}^{p'} \propto \mu_{j}^{p'}$. In addition, if one averages over all possible lab-fixed coordinate systems,[22,45] then one obtains

$$r(t) = \frac{1}{5}\left(\frac{3\left\langle \sum_{j}\left|\sum_{i}(\vec{\mu}_{i}(0)\cdot\vec{\mu}_{j}(t))U_{ji}(t)\right|^{2}\right\rangle}{\left\langle \sum_{j}|\vec{\mu}_{j}(t)|^{2}\left|\sum_{i}\vec{\mu}_{i}(0)U_{ji}(t)\right|^{2}\right\rangle} - 1\right). \tag{A9}$$

This formula contains the products $U_{ji}(t)U_{jk}(t)^{*}$. When averaged over the ensemble, these products of oscillating propagator elements, will, to an excellent approximation, vanish unless $i = k$. Keeping only these diagonal terms, we obtain

$$r(t) = \frac{1}{5}\left(\frac{3\left\langle \sum_{j}\sum_{i}(\vec{\mu}_{i}(0)\cdot\vec{\mu}_{j}(t))^{2}\left|U_{ji}(t)\right|^{2}\right\rangle}{\left\langle \sum_{j}\sum_{i}|\vec{\mu}_{i}(0)|^{2}|\vec{\mu}_{j}(t)|^{2}\left|U_{ji}(t)\right|^{2}\right\rangle} - 1\right). \tag{A10}$$

Using $\vec{\mu}_{i}(t) = \hat{u}_{i}(t)m_{i}(t)$, and the definition of the second Legendre polynomial ($P_{2}(x) = (3x^{2} - 1)/2$), we obtain Eq. (9).

APPENDIX B: DERIVATION OF THE FÖRSTER SURVIVAL PROBABILITY

The Förster result for the survival probability comes from considering a donor chromophore fixed in space, with randomly distributed acceptors. One assumes a master equation for incoherent and irreversible excitation transport

$$\dot{P}_{i}(t) = -\sum_{j} k_{ij}P_{i}(t), \tag{B1}$$

where $P_{i}(t)$ is the probability of finding the excitation on donor chromophore i at time t, and k_{ij} is the rate constant for energy transfer from chromophore i to j.

Assuming that dipole-dipole interactions are responsible for the energy transfer, the rate constant, within perturbation theory in the coupling, has the form

$$k_{ij} = \frac{3}{2}\frac{\kappa_{ij}^{2}}{\tau}\left(\frac{r_{o}}{r_{ij}}\right)^{6}, \tag{B2}$$

as in Eq. (14). Typically, one then *pre-averages* the orientation factor to arrive at a orientation-independent rate constant. Assuming random orientations gives $\langle\kappa^{2}\rangle = 2/3$,[14] and so, the pre-averaged rate constant is[9]

$$k_{ij} = \frac{1}{\tau}\left(\frac{r_{o}}{r_{ij}}\right)^{6}. \tag{B3}$$

The trivial solution to the master equation, subject to the initial condition that $P_i(0) = 1$, is

$$P_i(t) = e^{-\sum_j k_{ij} t} = \prod_j e^{-k_{ij} t}. \tag{B4}$$

The survival probability is the average of $P_i(t)$ over all configurations of acceptors

$$S(t) = \left\langle \prod_j e^{-k_{ij} t} \right\rangle = \langle e^{-k_{ij} t} \rangle^N, \tag{B5}$$

where N is the number of chromophores. The second equation follows from the assumption of randomly distributed chromophores. This can be written as

$$S(t) = \left[1 - \frac{N \langle 1 - e^{-k_{ij} t} \rangle}{N} \right]^N, \tag{B6}$$

which as the thermodynamic limit is approached is

$$S(t) = e^{-N \langle 1 - e^{-k_{ij} t} \rangle}. \tag{B7}$$

Note that a similar approach was used by Tachiya in his derivation of the rate constant for diffusion-controlled reactions.[46] Again, assuming randomly distributed acceptors, the exponent is given by

$$N \langle 1 - e^{-k_{ij} t} \rangle = \frac{N}{V} \int_0^{R_c} 4\pi r^2 dr (1 - e^{-(t/\tau)(r_o/r)^6}), \tag{B8}$$

where $V = 4\pi R_c^3/3$ is the volume. In the thermodynamic limit, this is

$$N \langle 1 - e^{-k_{ij} t} \rangle = 4\pi\rho \int_0^{\infty} r^2 dr (1 - e^{-(t/\tau)(r_o/r)^6}), \tag{B9}$$

where $\rho = N/V$ is the number density of acceptors. Letting $x = r^3$, this can be integrated to obtain[14]

$$S(t) = \exp\left(-\frac{4\pi^{3/2}\rho}{3} \sqrt{\frac{t r_o^6}{\tau}} \right). \tag{B10}$$

APPENDIX C: SURVIVAL PROBABILITY WITH REVERSIBLE ENERGY TRANSFER

If the energy transfer is reversible, then one needs to solve the full master equation. Taking the pre-averaged rate constant from above, this is

$$\dot{P}_i(t) = -\sum_j k_{ij} P_i(t) + \sum_j k_{ji} P_j(t), \tag{C1}$$

where $k_{ij} = k_{ji}$.

Suppose that we first consider the donor with only a single acceptor. Then, the solution of the master equation with initial excitation on site i is

$$P_i(t) = \frac{1 + e^{-2k_{ij} t}}{2}. \tag{C2}$$

One next approximates the survival probability for the many-acceptor system by[14,18]

$$P_i(t) = \prod_j \frac{1 + e^{-2k_{ij} t}}{2}. \tag{C3}$$

Note that while this gives the correct result that $P_i(0) = 1$, if there are N acceptors it gives the incorrect result that $P_i(\infty) = 1/2^N$ (the correct result is $P_i(\infty) = 1/N$).

Nonetheless, if we now take the ensemble average, we can write the survival probability as

$$S(t) = \left[1 - \frac{1}{2} \langle 1 - e^{-2k_{ij} t} \rangle \right]^N \simeq e^{-(N/2)\langle 1 - e^{-2k_{ij} t} \rangle}. \tag{C4}$$

Following the derivation in Appendix B, one then arrives at Eq. (19).

APPENDIX D: THE GENERALIZED FÖRSTER ENERGY TRANSFER

Here, we relax the assumption that the acceptors have random positions and orientations. We begin by pre-averaging the orientation factor for those chromophores at a given distance, and so, the rate constant becomes

$$k_{ij} = \frac{3}{2} \frac{\langle \kappa^2 \rangle_{r_{ij}}}{\tau} \left(\frac{r_0}{r_{ij}} \right)^6, \tag{D1}$$

where as shown, $\langle \kappa^2 \rangle_r$ depends on the distance between the chromophores. The derivation then follows that in Appendix B, except now Eq. (B9) becomes

$$N \langle 1 - e^{-k_{ij} t} \rangle = 4\pi\rho \int_0^{\infty} r^2 g(r) dr (1 - e^{-(t/\tau)(3/2)\langle \kappa^2 \rangle_r (r_o/r)^6}). \tag{D2}$$

If we now consider reversible energy transfer, then the survival probability becomes

$$S(t) = \exp\left(-2\pi\rho \int_0^{\infty} r^2 g(r) dr (1 - e^{-(t/\tau) 3 \langle \kappa^2 \rangle_r (r_o/r)^6}) \right). \tag{D3}$$

[1] S. Jang, J. Chem. Phys. **127**, 174710 (2007).
[2] S. Jang, Y.-C. Cheng, D. R. Reichman, and J. D. Eaves, J. Chem. Phys. **129**, 101104 (2008).
[3] B. M. Auer and J. L. Skinner, J. Chem. Phys. **128**, 224511 (2008).
[4] M. Yang and J. L. Skinner, Phys. Chem. Chem. Phys. **12**, 982 (2010).
[5] C. J. Fecko, J. J. Loparo, S. T. Roberts, and A. Tokmakoff, J. Chem. Phys. **122**, 054506 (2005).
[6] Y. L. A. Rezus and H. J. Bakker, J. Chem. Phys. **125**, 144512 (2006).
[7] S. Woutersen and H. J. Bakker, Nature (London) **402**, 507 (1999).
[8] D. Kraemer, M. L. Cowan, A. Paarmann, N. Huse, E. T. J. Nibbering, T. Elsaesser, and R. J. D. Miller, Proc. Natl. Acad. Sci. U.S.A. **105**, 437 (2008).
[9] L. Piatkowski, K. B. Eisenthal, and H. J. Bakker, Phys. Chem. Chem. Phys. **11**, 9033 (2009).
[10] T. Förster, Z. Naturforsch. **4**, 821 (1940).
[11] G. D. Scholes, Annu. Rev. Phys. Chem. **54**, 57 (2003).
[12] G. R. Fleming and G. D. Scholes, Nature (London) **431**, 256 (2004).
[13] S. Jang, M. D. Newton, and R. J. Silbey, Phys. Rev. Lett. **92**, 218301 (2004).
[14] J. Baumann and M. D. Fayer, J. Chem. Phys. **85**, 4087 (1986).
[15] M. Yang and G. R. Fleming, Chem. Phys. **282**, 163 (2002).
[16] S. W. Haan and R. Zwanzig, J. Chem. Phys. **68**, 1879 (1978).
[17] C. R. Gochanour, H. C. Andersen, and M. D. Fayer, J. Chem. Phys. **70**, 4254 (1979).
[18] D. L. Huber, D. S. Hamilton, and B. Barnett, Phys. Rev. B **16**, 4642 (1977).
[19] H. Bakker and J. L. Skinner, Chem. Rev. **110**, 1498 (2010).
[20] J. L. Skinner, B. M. Auer, and Y.-S. Lin, Adv. Chem. Phys. **142**, 59 (2009).
[21] B. M. Auer, R. Kumar, J. R. Schmidt, and J. L. Skinner, Proc. Natl. Acad. Sci. U.S.A. **104**, 14215 (2007).
[22] Y.-S. Lin, P. A. Pieniazek, M. Yang, and J. L. Skinner, J. Chem. Phys. **132**, 174505 (2010).

[23]F. Li and J. L. Skinner, J. Chem. Phys. **132**, 204505 (2010).
[24]F. Li and J. L. Skinner, J. Chem. Phys. **133**, 244504 (2010).
[25]B. M. Auer and J. L. Skinner, J. Chem. Phys. **129**, 214705 (2008).
[26]B. M. Auer and J. L. Skinner, J. Phys. Chem. B **113**, 4125 (2009).
[27]P. A. Pieniazek, C. J. Tainter, and J. L. Skinner, J. Am. Chem. Soc. **133**, 10360 (2011).
[28]P. A. Pieniazek, C. J. Tainter, and J. L. Skinner, J. Chem. Phys. **135**, 044701 (2011).
[29]Y.-S. Lin, B. M. Auer, and J. L. Skinner, J. Chem. Phys. **131**, 144511 (2009).
[30]P. A. Pieniazek, Y.-S. Lin, J. Chowdhary, B. M. Ladanyi, and J. L. Skinner, J. Phys. Chem. B **113**, 15017 (2009).
[31]S. M. Gruenbaum and J. L. Skinner, J. Chem. Phys. **135**, 075101 (2011).
[32]T. L. C. Jansen, B. M. Auer, M. Yang, and J. L. Skinner, J. Chem. Phys. **132**, 224503 (2010).
[33]H. J. C. Berendsen, J. R. Grigera, and T. P. Straatsma, J. Phys. Chem. **91**, 6269 (1987).
[34]G. R. Fleming, *Chemical Applications of Ultrafast Spectroscopy* (Oxford University Press, New York, 1986).
[35]I. R. Piletic, D. E. Moilanen, D. B. Spry, N. E. Levinger, and M. D. Fayer, J. Phys. Chem. A **110**, 4985 (2006).
[36]H. J. Bakker, Y. L. A. Rezus, and R. L. A. Timmer, J. Phys. Chem. A **112**, 11523 (2008).
[37]N. E. Levinger and L. A. Swafford, Annu. Rev. Phys. Chem. **60**, 385 (2009).
[38]S. Mukamel, *Principles of Nonlinear Optical Spectroscopy* (Oxford, New York, 1995).
[39]T. L. C. Jansen and J. Knoester, J. Phys. Chem. B **110**, 22910 (2006).
[40]J. R. Schmidt, S. A. Corcelli, and J. L. Skinner, J. Chem. Phys. **123**, 044513 (2005).
[41]A. Paarmann, T. Hayashi, S. Mukamel, and R. J. D. Miller, J. Chem. Phys. **128**, 191103 (2008).
[42]A. Paarmann, T. Hayashi, S. Mukamel, and R. J. D. Miller, J. Chem. Phys. **130**, 204110 (2009).
[43]T. Schäfer, J. Lindner, P. Vöhringer, and D. Schwarzer, J. Chem. Phys. **130**, 224502 (2009).
[44]G. Stock and W. Domcke, Phys. Rev. A **45**, 3032 (1992).
[45]D. A. McQuarrie, *Statistical Mechanics* (Harper and Row, New York, 1976).
[46]M. Tachiya, Radiat. Phys. Chem. **21**, 167 (1983).